

Research

Intrafraction Motion Management in Cyberknife SRS with 6D-Skull Tracking

Kushal Narang^{1*}, Tejinder Kataria¹ and Deepak Gupta¹

¹Division of Radiation Oncology, Medanta Cancer institute, Medanta The Medicity, Sector 38, Gurgaon, Haryana, India – 122001

Abstract

Purpose

Initial evaluation of intrafraction motion in patients with intracranial targets treated with frameless, mask based stereotactic radio surgery (SRS) using 6D-skull tracking on CyberKnife.

Methods and Materials

Datasets of five patients with intracranial targets treated with CyberKnife VSI using customized, non-invasive frameless thermoplastic cast based immobilization were analyzed. Standard CyberKnife couch for correcting positional offsets and 6D-skull tracking for detecting and correcting intrafraction shifts was used. For each sequential pair of images, the correction to the target position (position “offset”) was determined in six-degrees of motion (3 translations and 3 rotations). In all, 175 intrafraction positional offsets were analyzed to calculate the intrafraction shifts. Mean shifts, standard deviations, and range of shifts were estimated.

Results

The mean and 1 standard deviation (SD) intrafraction translational shifts were 0.12±0.16mm in left-right direction, 0.14±0.25mm in antero-posterior direction and 0.12±0.13mm in supero-inferior direction. The mean and 1 SD intrafraction rotational shifts were 0.08±0.24 degrees roll, 0.12±0.17 degrees pitch and 0.14±0.13 degrees yaw. Although translational shifts ranged between +3.3 mm to -2.9 mm, and rotational shifts between +0.8 degrees to -1.3 degrees, most (> 99%) of the shifts were < 1 mm and 1 degree.

Conclusion

CyberKnife SRS with frameless thermoplastic mask based immobilization and 6D-skull tracking, effectively detects and compensates for intrafraction motion. One mm PTV margin appears sufficient to account for most of this motion.

Keywords: CyberKnife; 6-D Skull Tracking; Intrafraction Motion

Introduction

Stereotactic radio surgery (SRS) and radiotherapy (SRT) are techniques that deliver radiation in high dose single and multiple fractions, respectively, with a high degree of conformality. The sharp gradient between the target edge and normal tissue necessitates a high level of precision, for optimizing tumour control and minimizing normal tissue toxicity. Clinical experience over the past five decades has led to appropriate titration of doses and fractionation as well, in order to maintain a favorable therapeutic ratio.

All SRS / SRT deliveries essentially require strict immobilization of the head, while ensuring patient comfort, and set-up reproducibility. An accuracy of within 1-2 mm and overall geometric and dosimetric uncertainty within 2% is typically recommended [1]. The comparable levels of interfraction reproducibility shown by frameless techniques coupled with image guidance, and the impracticality of using rigid frames for SRT, have led to increased use of the former for both SRS and SRT [2-4]. We have ourselves demonstrated the comparable reproducibility of Linear Accelerator (LINAC) based frameless radio surgery at our institute [5]. However, there is no way to limit the intrafraction motion with the frameless technique apart from stringent intrafraction imaging, and hence, the need to assess the effectiveness of the same is vital.

Initial encouraging experience for intracranial lesions treated with SRS/SRT on Gamma Knife (GK) [6] and subsequently on LINAC [7, 8] has paved the way for its execution on the highly advanced robotic radiation delivery system, the CyberKnife (CK). This machine uses a 6-MV LINAC mounted on a fully articulated robotic arm with six degrees of freedom, which allows targeting lesions from a much wider variety of angles than on a conventional LINAC [9]. Moreover, the processes of calculation of positional shifts and their correction, intrafraction imaging and tumour tracking are fully automated. The purpose of the present study is to demonstrate the magnitude of intrafraction motion in intracranial cases treated with thermoplastic mask based frameless SRS coupled with 6D-skull tracking on the CyberKnife® VSI Radiosurgery System (Accuray Inc., Sunnyvale, CA, USA).

Materials and Methods

Five patients treated with SRS on the CyberKnife® Radio surgery System (Accuray Inc., Sunnyvale, CA, USA) were identified as

***Corresponding author:** Kushal Narang, Division of Radiation Oncology, Medanta Cancer Institute, Medanta the Medicity, Sector 38, Gurgaon, Haryana, India – 122001, Tel: +918588896979; Fax: +911244834111; E-mail: narangkushal@gmail.com

Sub Date: May 15, 2015, **Acc Date:** June 11, 2015, **Pub Date:** June 11, 2015.

Citation: Kushal Narang, Tejinder Kataria and Deepak Gupta (2016) Intrafraction Motion Management in Cyberknife SRS with 6D-Skull Tracking. BAOJ Neuro 1: 005.

Copyright: © 2016 Kushal Narang, et al. This is an open-access article distributed under the terms of the Creative Commons Attribution License, which permits unrestricted use, distribution, and reproduction in any medium, provided the original author and source are credited.

subjects for the study. Patients were immobilized in supine position using a customized, non-invasive uniframe thermoplastic cast, with soft foam for head support and soft mattress for body support. Subsequently, they underwent a non-contrast treatment planning CT scan of the head (1 mm slice thickness, without superposition of slices, 512×512 matrix, and pitch of 1). No fiducial markers were used because of the capability of image based couch correction by CK at set up. After this, patients underwent a contrast-enhanced T1-weighted MRI (26 cm FOV, 512×512 pixel size, 1 mm slice interval) using a 1.5 Tesla MRI. The target volume delineation on the fused CT and MRI images, and dose/fractionation selection based on the tumor size, tumour location/ proximity to critical structures and previous treatment (surgery, radiotherapy or both) was done jointly by the radiation oncologist and neurosurgeon. SRS was selected to treat patients only if the tumors were smaller than 3 cm.

The gross tumor volume (GTV) was delineated as contrast-enhancing tumor demonstrated on MRI scans. Clinical target volume (CTV) was either the same as GTV, or constructed with an appropriate margin on a case-by-case basis. No Planning target volume (PTV) was required.

The equivalent 2 Gy dose (EQD2) was calculated according to the formula, $EQD2 = n \times d \times (\alpha/\beta + d) / (\alpha/\beta + 2)$. Inverse planning was used to determine the dose to the target volume while minimizing the dose to normal tissues using the Multiplan software (Accuray Inc., Sunnyvale, CA, USA). An optimal treatment plan was expected to deliver SRS to the 80%-90% is dose line encompassing 100 % of the PTV. Target coverage, dose heterogeneity and conformality index were examined to evaluate the quality of treatment plans. Strict quality assurance was done to ensure smooth execution of the treatment plan on the machine.

The CyberKnife frameless radio surgery system uses a 6-MV LINAC mounted on a fully articulated robotic arm with six degrees of freedom. The robot can correct translations of up to ± 10 mm and rotations of up to $\pm 1^\circ$ roll and pitch, and $\pm 3^\circ$ yaw [9]. Multiple digitally reconstructed radiographs (DRRs) are generated by the planning system before treatment. During treatment, two orthogonally positioned x-ray detectors provide almost real-time imaging of bony anatomy, thus allowing intrafraction shift correction. The system enables the user to specify the minimum interval between image acquisitions within a range of 5 - 150 seconds during treatment. When acquisition starts, a default image interval is selected. After verifying target stability for the first few minutes, the imaging interval can be increased progressively up to a 60 seconds minimum, depending on patient stability [9]. Using complex tracking algorithms, each projection is co-registered with the reference DRR image in six-dimensional space, thus providing data on the patient motion during treatment.

For treatment, the patient with the thermoplastic cast assembly

was positioned on the treatment couch in an identical manner as per CT simulation. Check imaging was done to detect positional translational and rotational shifts, which were then corrected by couch movement. 6D skull tracking based on the two-dimensional (2D)-three-dimensional (3D) image registration method, as described by Fu, et al [10] was done. The 2D-3D image registration method measures translations and rotations of the skull by comparing two acquired orthogonal views of the skull silhouette with the DRRs, and thus determines the target position at the given time-point during treatment. The frequency of X-Ray imaging was set at approximately every 30 to 40 seconds, and was adjusted according to the target position during treatment. The intrafraction rotational and translational positional shifts so determined were simultaneously corrected by the movement of the robot. In case the intrafraction shifts were beyond the limits of correction by the robot, couch shifts were used to correct the same. Fig 1 depicts the CyberKnife treatment console, with a fraction in progress.

The complete details of the positional offset values and the consequent robotic movements required to correct them during treatment are recorded as system log files. The individual patient dataset consists of translational offsets in lateral or left-right (LR) direction, antero-posterior (AP) direction and supero-inferior (SI) direction, and rotational offsets as roll, pitch and yaw. These datasets were then screened for offsets due to manual couch movement during set-up phase or in-between treatment, and these were excluded from the analysis. The actual intrafraction shifts in each direction were calculated by subtracting a particular offset value (n) from the immediately succeeding one (n + 1), as follows :

Translations

$$\begin{aligned} \Delta X_1 &= X_{n+1} - X_n & \Delta Y_1 &= Y_{n+1} - Y_n & \Delta Z_1 &= Z_{n+1} - Z_n \\ \Delta X_2 &= X_{n+2} - X_{n+1} & \Delta Y_2 &= Y_{n+2} - Y_{n+1} & \Delta Z_2 &= Z_{n+2} - Z_{n+1} \\ \Delta X_3 &= X_{n+3} - X_{n+2} & \Delta Y_3 &= Y_{n+3} - Y_{n+2} & \Delta Z_3 &= Z_{n+3} - Z_{n+2} \dots \text{ and} \\ & & & & & \text{so on} \end{aligned}$$

Rotations

$$\begin{aligned} \Delta R_1 &= R_{n+1} - R_n & \Delta P_1 &= P_{n+1} - P_n & \Delta YW_1 &= YW_{n+1} - YW_n \\ \Delta R_2 &= R_{n+2} - R_{n+1} & \Delta P_2 &= P_{n+2} - P_{n+1} & \Delta YW_2 &= YW_{n+2} - YW_{n+1} \\ \Delta R_3 &= R_{n+3} - R_{n+2} & \Delta P_3 &= P_{n+3} - P_{n+2} & \Delta YW_3 &= YW_{n+3} - YW_{n+2} \dots \\ & & & & & \text{and so on} \end{aligned}$$

Where

ΔX_1 is the first intrafraction shift in the Left-Right (LR) direction, X_{n+1} and X_n are the second and first positional offsets, respectively, in the LR direction

ΔY_1 is the first intrafraction shift in the Antero-Posterior (AP) direction, Y_{n+1} and Y_n are the second and first positional offsets, respectively, in the AP direction

ΔZ_1 is the first intrafraction shift in the X Supero-inferior (SI) direction, Z_{n+1} and Z_n are the second and first positional offsets, respectively, in the SI direction

ΔR_1 is the first intrafraction shift in Roll, R_{n+1} and R_n is the second and first positional offsets, respectively, in the Roll

ΔP_1 is the first intrafraction shift in Pitch, P_{n+1} and P_n are the second and first positional offsets, respectively, in the Pitch

ΔYW_1 is the first intrafraction shift in Yaw, YW_{n+1} and YW_n are the second and first positional offsets, respectively, in the Yaw

The range of all intrafraction shifts in the “+” and “-“directions was noted. For calculation of mean shifts, the dataset of intrafraction shifts was converted to “all-positive” values by eliminating the minus sign. This was done so as to avoid the “+” and “-“shifts mutually cancelling out each other while calculating the mean shifts. Mean intrafraction shifts and Standard Deviations were then calculated from this all positive value dataset for each translational and rotational direction, individually for each patient and also as the pooled dataset of all five patients. All statistical analyses were performed using Microsoft Office Excel version 2007.

Results

The various lesions treated included Cranial Arterio-Venous Malformations (n = 2), Cerebellopontine angle Schwannoma (n = 1), Meningioma (n = 1) and single brain metastasis (n = 1). Mean treatment time for daily fraction was 39 minutes (range from 33 to 45 minutes). Mean imaging interval during delivery of a fraction was 37.2 seconds. The mean intrafraction translational errors recorded for all patients were 0.12 mm (SD ± 0.16 mm) in the LR direction, 0.14 mm (SD ± 0.25 mm) in the AP direction, and 0.12 mm (SD ± 0.13 mm) in the S-I direction. The rotational positioning errors were 0.08 degree roll (SD ± 0.24 degree), 0.12 degree pitch (SD ± 0.17 degree), and 0.14 degree yaw (SD ± 0.13 degree). The individual mean intrafraction errors for the 5 SRS fractions are listed in Table 1. Fig 2 depicts an example of the intrafraction shifts for a patient, and Figures 3 and 4 depict the range of shifts for translations and rotations for the 5 SRS treatment fractions.

Discussion

Since the late sixties when the first cranial radio surgery was done on Leksell's Gamma Knife [6], different intracranial lesions have been treated with SRS / SRT with varying levels of accuracy. Improvements in radiation technology and physics have been ably supported by intelligent use of principles of radiation biology to attain the therapeutic aim [11, 12]. Besides GK, SRS / SRT have been increasingly practiced on LINAC and more recently on CK. Although there are no randomized comparisons of the incidence of neurotoxicity between conventional or conformal radiation techniques on LINAC versus the CK, the switch is largely based on the latter's technological superiority. With the abilities to target lesions from virtually any angle in three-dimensional space, to track the intrafraction motion of the target, and to compensate for the same, the CK requires no or minimal PTV margins for carrying out SRS and SRT. This, in turn, translates into a very minimal irradiation of the normal brain, and consequently, a definite reduction in neurotoxicity. The clinical significance of reduced treatment margins in SRS has been evaluated by Nataf et al [13]. In their study, the clinical and planning target volumes margin was enlarged from 1 to 2 mm, and significantly more severe parenchymal complications (p = 0.02) occurred within a group of 93 patients with brain metastases. They recommended reduction of the margin to 1 mm for minimization of complications. Clinical experience with CyberKnife SRS / SRT for the treatment of brain metastases by Murai et al [14], and by Inoue et al [15] have not reported any incidence of Grade III or higher neurotoxicity. Inoue et al [15] further concluded that the incidence of symptomatic brain necrosis could be eliminated by restricting V14 of normal brain to < 7 cc, when treating brain metastases with three fractions CK.

With minimal margin for error, an accurate and reproducible immobilization of head naturally becomes fundamental to the delivery of SRS and SRT. Though the same required a rigid cranial frame in the past, now diverse frameless devices are available, such as implanted fiducial markers and infrared camera guidance that

Table 1: Intrafraction Shifts of 5 SRS* fractions

SI No	Mean L/R [†] shift ± SD [§] (mm)	Mean A/P [‡] shift ± SD [§] (mm)	Mean S/I [§] shift ± SD [§] (mm)	Mean Roll ± SD [§] (degrees)	Mean Pitch ± SD [§] (degrees)	Mean Yaw ± SD [§] (degrees)
1	0.09 ± 0.09	0.12 ± 0.15	0.09 ± 0.10	0.03 ± 0.05	0.09 ± 0.08	0.13 ± 0.15
2	0.15 ± 0.22	0.07 ± 0.11	0.10 ± 0.10	0.05 ± 0.07	0.13 ± 0.13	0.13 ± 0.13
3	0.12 ± 0.16	0.16 ± 0.17	0.13 ± 0.13	0.08 ± 0.08	0.13 ± 0.23	0.13 ± 0.15
4	0.15 ± 0.17	0.22 ± 0.41	0.15 ± 0.16	0.13 ± 0.44	0.14 ± 0.22	0.15 ± 0.13
5	0.08 ± 0.09	0.09 ± 0.10	0.14 ± 0.16	0.07 ± 0.15	0.07 ± 0.06	0.13 ± 0.10
	0.12 ± 0.16	0.14 ± 0.25	0.12 ± 0.13	0.08 ± 0.24	0.12 ± 0.17	0.14 ± 0.13

*SRS : Stereotactic Radiosurgery

[†]L/R: Left-Right; [‡]A/P : Antero-Posterior; [§]S/I : Supero-Inferior

[§]SD : Standard Deviation



Fig 1: depicts the CyberKnife treatment console, with a fraction in progress.

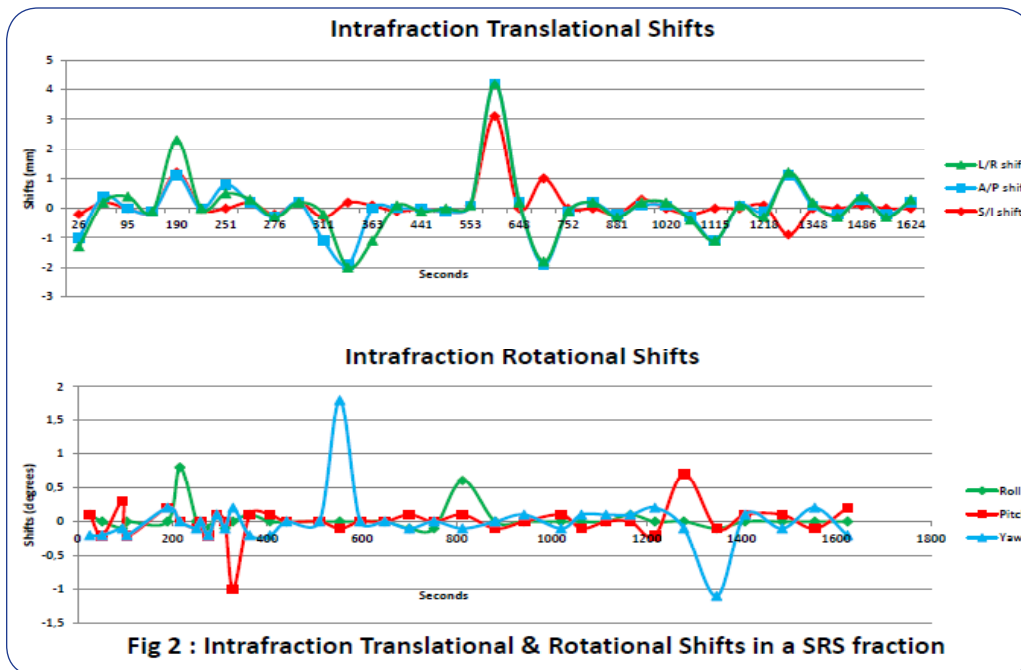
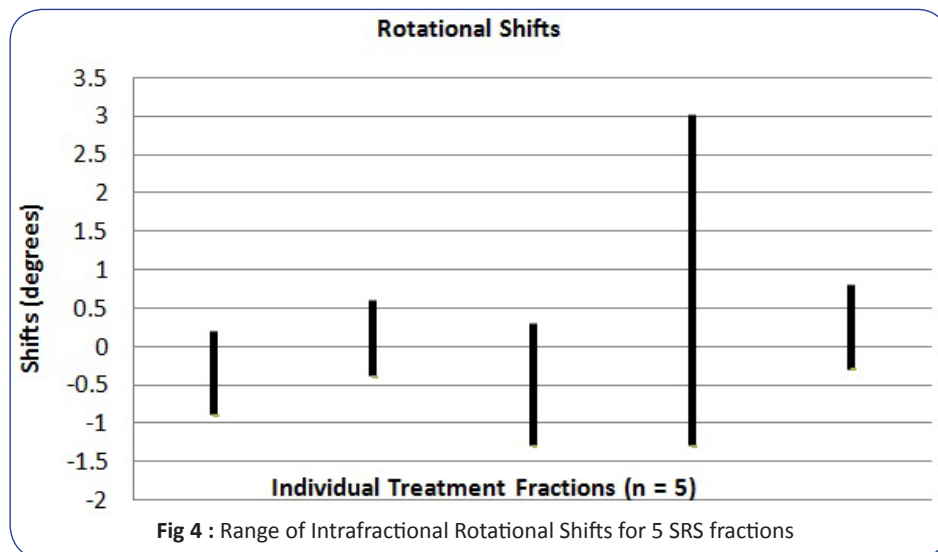
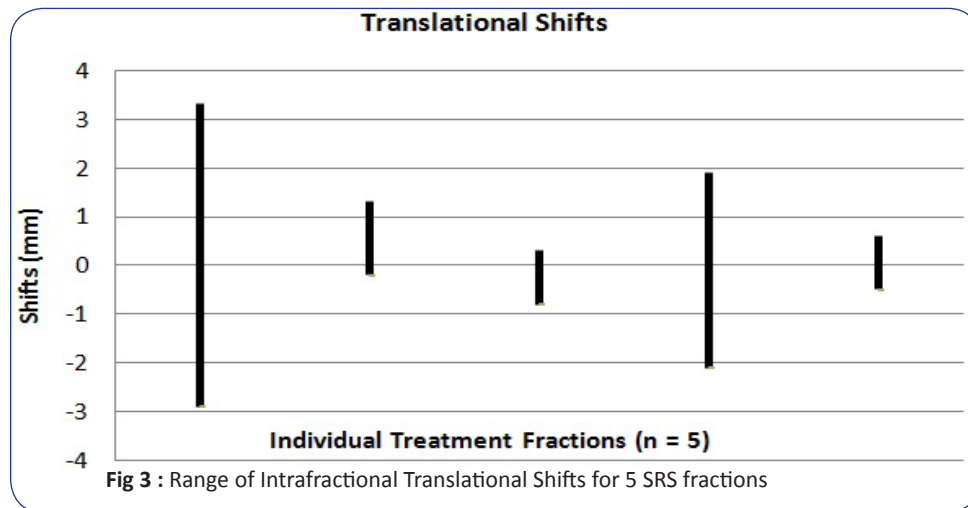


Fig 2 : Intrafraction Translational & Rotational Shifts in a SRS fraction



have shown comparable accuracy as frame based techniques for minimizing interfraction movement [16]. Based on the results in literature [17], and that of our own study [5], we believe that a well constructed thermoplastic mask with dedicated image guidance in real time during treatment serves the purpose equally well. This, however, is not sufficient to minimize intrafraction motion. While carrying out LINAC based frameless SRS, we obtained mean intrafraction translational shifts as 0.40 ± 0.90 mm, 1.10 ± 1.10 , and 0.50 ± 1.30 mm in L-R, A-P, and S-I directions, respectively, and rotational shifts as 0.11 ± 0.78 , 0.20 ± 0.44 , and 0.29 ± 0.35 degrees in roll, pitch, and yaw, respectively [5], which are visibly greater than those obtained on CK in the present study.

Till date, most of such studies assessing intrafraction motion have been performed for LINAC based radio surgery, relying on pre- and post-treatment imaging as a surrogate. Badakshi, et al [18] also performed measurements at several time points during the course of treatment and found that 12% of the intrafraction values in the three dimensions were above the usual safety margin

of 1 mm typically applied in SRS. Murphy [19] and Hoogeman [20] assessed intrafraction motion on CK, and calculated margins based on the relation proposed by van Herk et al [21]. Floriano, et al [22] reported their experience of cranial SRS / SRT on CK with a 99% displacement error less than 0.85 mm, systematic intrafraction movement components less than 0.05 mm and random intrafraction movement components less than 0.3 mm in the 3 translational axes, with a linear time dependence in the random component. Murphy et al [23] examined patterns of patient movement during frameless image-guided radio surgery and found that the mean translational difference was 0.45 mm per axis. Inoue, et al [24] assessed the effect of residual patient motion on dose distribution during intracranial image-guided robotic radio surgery, and reported median translational residual patient motion as 0.1 mm for each axis, and rotational residual patient motion as 0.1 degree for pitch and roll and 0.2 degree for yaw. The dose error for D95 was reported as within 1 % in more than 95 % of cases, and the maximum dose error for D10 to D90 was within 2 %. Kang, et al

[25] examined the dosimetric impact of intrafraction movements occurring during image-guided frameless brain radiosurgery and attempted to derive optimal margins required to compensate the movement. They derived the formula $1.0r + 0.2\sigma$, where r and σ are the average and standard deviation of the movements, respectively. They calculated that the optimal margins for treatment times of 10, 20, and 30 min were 2.1, 3.2, and 4.2 mm, respectively, at 90% confidence level.

In our study, we have evaluated the accuracy in terms of translational and rotational uncertainties on CK using intra-treatment X-ray verification using 6D-skull tracking. The observed mean translational and rotational shifts were all less than 0.2 mm. These are comparable to the shifts obtained in the study by Inoue et al [24] and much lesser than some of the earlier studies mentioned above [19, 20, 22, 23]. As explained by Inoue, et al, this difference might be attributable to the interval between acquiring sequential images and the type of imaging system used in each study. The mean interval between sequential images was 37.2 s in our study, which was much lesser than the mean interval of 120 s in the study by Murphy et al [23]. Also, improved imaging quality as provided by the amorphous silicon diode detectors, over and above the X-ray image intensifiers used earlier, also accounts for the lesser intrafraction shifts.

However, even though the mean frequency of imaging was 37.2 seconds, it is still not real-time in the strict sense, and the targeting error between two successive image acquisitions is used as surrogate for intrafraction motion. Thus, the study still fails to detect and evaluate the impact of transient motion, such as swallowing. However, as all our cases had intracranial targets, the impact of transient motion should not be a factor significant enough to alter the results obtained.

Since this is an initial evaluation, small patient numbers is definitely a drawback. This was intended to be a study describing the CK methodology at our institute and to assess and analyze the pattern of intrafraction motion on CK. A larger dataset shall subsequently be analyzed to substantiate the results. Different histologies of brain lesions were evaluated, and while this may have a bearing on the clinical outcome, we do not believe that this may alter the pattern of intrafraction motion of targets in any way. However, the location of the lesion within the brain (high frontal versus deep parenchymal versus close to base of skull) may produce differences in the pattern of intrafraction motion, depending on the effectiveness of immobilization and overall patient stability.

Conclusion

In our experience, intrafraction motion for intracranial targets treated with fiducial free, frameless cranial SRS / SRT on CyberKnife with 6-D skull tracking, is within the acceptable range, and can be reliably detected and corrected.

References

1. Benedict SH, Yenice KM, Followill D (2010) Stereotactic body radiation therapy: The report of AAPM Task Group 101. *Med Phys* 37(8):4078-4101.

- Lamba M, Breneman JC, Warnick RE (2009) Evaluation of image-guided positioning for frameless intracranial radiosurgery. *Int J Radiat Oncol Biol Phys* 74(3): 913-919.
- Gevaert T, Verellen D, Tournel K (2012) Setup accuracy of the Novalis ExacTrac 6DOF system for frameless radiosurgery. *Int J Radiat Oncol Biol Phys* 82(5): 1627-1635.
- Karger CP, Jakel O, Debus J, Kuhn S, Hartmann GH, et al. (2001) Three-dimensional accuracy and interfractional reproducibility of patient fixation and positioning using a stereotactic head mask system. *Int J Radiat Oncol Biol Phys* 49(5): 1493-504.
- Kataria T, Gupta D, Karrthick KP (2013) Frame-based radiosurgery: Is it relevant in the era of IGRT? *Neurol India* 61(3): 277-281.
- Leksell L (1983) Stereotactic Radiosurgery. *J Neurol Neurosurg Psychiatr* 46(9): 797-803.
- Buatti JM, Bova FJ, Friedman WA (1998) Preliminary experience with frameless stereotactic radiotherapy. *Int J Radiat Oncol Biol Phys* Oct 42(3): 591-599.
- Rosenthal SJ, Gall KP, Jackson M, Thornton AF Jr (1995) A precision cranial immobilization system for conformal stereotactic fractionated radiation therapy. *Int J Radiat Oncol Biol Phys* 33(1): 1239-1245.
- Dieterich S, Gibbs IC (2011) The CyberKnife in clinical use: current roles, future expectations. *Front Radiat Ther Oncol* 43: 181-194.
- Fu D, Kuduvali G (2008) A fast, accurate, and automatic 2D-3D image registration for image-guided cranial radiosurgery. *Med Phys* 35(5): 2180-2194.
- Flickinger JC, Kondziolka D, Lunsford LD (2000) Development of a model to predict permanent symptomatic postradiosurgery injury for arteriovenous malformation patients. Arteriovenous Malformation Study Group. *Int J Radiat Oncol Biol Phys* 46(5): 1143-1148.
- Minniti G, Clarke E, Lanzetta G (2011) Stereotactic radiosurgery for brain metastases: Analysis of outcome and risk of brain radionecrosis. *Radiat Oncol* 6: 48.
- Nataf F, Schlienger M, Liu Z (2008) Radiosurgery with or without a 2-mm margin for 93 single brain metastases. *Int J Radiat Oncol Biol Phys* 70(3): 766-772.
- Murai T, Ogino H, Manabe Y (2014) Fractionated Stereotactic Radiotherapy using CyberKnife for the treatment of Large Brain Metastases: A dose escalation study. *Clinical Oncology* 26: 151-158.
- Inoue HK, Seto K, Nozaki A (2013) Three-fraction CyberKnife radiotherapy for brain metastases in critical areas: referring to the risk evaluating radiation necrosis and the surrounding brain volumes circumscribed with a single dose equivalence of 14 Gy (V14). *J Rad Res* 54: 727-735.
- Ramakrishna N, Rosca F, Friesen S, Tezcanli E, Zygmanski P, et al. (2010) A clinical comparison of patient setup and intra-fraction motion using frame-based radiosurgery versus a frameless image-guided radiosurgery system for intracranial lesions. *Radiation Oncol* 95(1): 109-115.
- Georg D, Bogner J, Dieckmann K, Potter R (2006) Is mask-based stereotactic head-and-neck fixation as precise as stereotactic head fixation for precision radiotherapy? *Int J Radiat Oncol Biol Phys* 66: S61-S66.

18. Badakhshi H, Barelkowski T, Wust P, Budach V, Boehmer D, et al. (2013) Intrafraction variations in linac-based image-guided radiosurgery of intracranial lesions. *Cancer Radiother* 17(7): 664-667.
19. Murphy MJ (2009) Intrafraction geometric uncertainties in frameless image-guided radiosurgery. *Int J Radiat Oncol Biol Phys* 73(5): 1364–1368.
20. Hoogeman MS, Nuyttens JJ, Levendag PC, Heijmen BJ (2008) Time dependence of intrafraction patient motion assessed by repeat stereoscopic imaging. *Int J Radiat Oncol Biol Phys* 70(2): 609–618.
21. Van Herk M, Remeijer P, Rasch C, Lebesque JV (2000) The probability of correct target dosage: Dose-population histograms for deriving treatment margins in radiotherapy. *Int J Radiat Oncol Biol Phys* 47(4): 1121-1135.
22. Floriano A, Santa Olalla I, Sanchez Reyes A (2013) Initial evaluation of intrafraction motion using frameless CyberKnife VSI system. *Rep Pract Oncol Radiother* 18(3): 173–178.
23. Murphy MJ, Chang SD, Gibbs IC (2003) Patterns of patient movement during frameless image-guided radiosurgery. *Int J Radiat Oncol Biol Phys* 55(5): 1400–1408.
24. Inoue M, Shiomi H, Sato K (2014) Effect of residual patient motion on dose distribution during image-guided robotic radiosurgery for skull tracking based on log file analysis. *Jpn J Radiol* 32(8): 461–466.
25. Kang KM, Chai GY, Jeong BK (2013) Estimation of optimal margin for intrafraction movements during frameless brain radiosurgery. *Med Phys* 40(5): 051716.